Journal of
Marine Science and Engineering

MDPI

Article

Semi-Automated Classification of Side-Scan Sonar Data for Mapping *Sabellaria spinulosa* Reefs in the Brown Bank, Dutch Continental Shelf

Timo Constantin Gaida [1,*], Bas Binnerts [1] and Oscar Bos [2]

[1] Department of Acoustic Signatures & Noise Control, TNO, 2597 AK Den Haag, The Netherlands; bas.binnerts@tno.nl
[2] Wageningen Marine Research, 1780 AB Den Helder, The Netherlands; oscar.bos@wur.nl
* Correspondence: timo.gaida@tno.nl

Abstract: Biogenic reefs support marine biodiversity and play a key role in a healthy marine environment. Protecting and enhancing reef-building species, such as *Sabellaria spinulosa*, require mapping and monitoring strategies. A multi-scale and multi-sensor mapping campaign, including a multi-beam echosounder, side-scan sonar (SSS), box corer and ROV with an attached video camera, has been carried out in the northern Brown Bank (Dutch Continental Shelf) in August 2023. A semi-automated classification workflow, based on a support vector machine (machine learning), was developed to map *Sabellaria* reefs using SSS and video data. Elevated *Sabellaria* reefs were classified with a precision and sensitivity of 52% and 49%, respectively. The classified SSS images were merged into full-coverage percentage maps of *Sabellaria* reef coverage. Located between the swales of the tidal ridges, it was estimated that the reefs cover an area of 3.8 to 5.7% within the surveyed areas. The maps indicate (1) on the large-scale a preference of *Sabellaria spinulosa* for settlement to the east of the deepest part of the swale and (2) on the small-scale a preference for the troughs towards the stoss side of the megaripples. The employed survey strategy and the developed classification workflow can be extended to other environmental areas and further developed into a standard monitoring procedure.

Keywords: side-scan sonar; acoustics; remote sensing; SVM; machine learning; computer vision; *Sabellaria spinulosa*; biogenic reefs; nature restoration

check for updates

Received: 11 November 2024
Revised: 12 December 2024
Accepted: 24 December 2024
Published: 3 January 2025

Citation: Gaida, T.C.; Binnerts, B.; Bos, O. Semi-Automated Classification of Side-Scan Sonar Data for Mapping *Sabellaria spinulosa* Reefs in the Brown Bank, Dutch Continental Shelf. *J. Mar. Sci. Eng.* **2025**, *13*, 74. https://doi.org/10.3390/jmse13010074

1. Introduction

Protecting and enhancing biogenic reef-forming species such as the Ross worm, *Sabellaria spinulosa*, is considered of key importance for North Sea nature restoration. While in English waters the presence of *Sabellaria* reefs is well-known, on the Dutch Continental Shelf (DCS) reefs were discovered for the first time in the Brown Bank area in 2017 [1]. In general, the chance of *Sabellaria* reef occurrence on the DCS is predicted to be low, with the highest chance in the Brown Bank area [1,2]. The biogenic reefs stabilize the seabed and potentially increase biodiversity by providing a habitat for a multitude of other species. Under OSPAR, a European regional sea convention for the protection of the marine environment of the North-East Atlantic, and within the Dutch Marine Strategy, these reefs are recognized to be under threat and in need of protection [3,4]. Therefore, it is important to map the current distribution of the reefs to help policymakers to develop effective protection measures [2].

Acoustic mapping techniques, such as the side-scan sonar (SSS) and multi-beam echosounder (MBES), allow to efficiently map large areas with a resolution on a centimetre to decimetre scale [5,6]. In the last decade, the MBES has become the sensor of choice for habitat mapping [7,8], whereas the majority of the SSS applications and its developments is related to object detection [9,10].

Methods for identifying *Sabellaria spinulosa* reefs have been reviewed by Limpenny et al. [11]. The SSS was mentioned as the most effective sensor, and guidance on optimizing the survey settings for the detection of *Sabellaria* reefs was provided. The importance of the SSS as a standard tool for mapping *Sabellaria* reefs was addressed by Jenkins et al. [12]. They present examples of SSS images with overlaying video tracks and show the presence of reefs and the corresponding acoustic pattern. Bianconi et al. [13] already took a step further and assessed the performance of texture-analysis methods to detect *Sabellaria* reefs from SSS images. The Gabor filter, a method based on Fourier analysis to highlight features with a certain pattern in an optical or acoustic image, was identified as the best method. The output of the texture analysis methods can then be fed into a classification workflow as a feature to enable the automated mapping of *Sabellaria* reefs. To the current knowledge of the authors, an automatic classification workflow for mapping *Sabellaria* reefs in a complex (heterogeneous) environment such as the Brown Bank has, however, not been presented.

The Brown Bank is relatively deep with 20 to 50 m and strong bathymetric variations and moderate tidal currents. These environmental conditions make it difficult to keep a stable vertical and horizontal SSS fish position, degrading the positional accuracy and the data quality of the sonar image. In addition, the Brown Bank has extensive distributions of megaripples with relatively short wavelengths (5 to 40 m) and large patches of shells [14]. The elevation of the megaripples causes a high reflectivity on the one side, similar as the shell beds, and on the other side an acoustic shadow. In such an environment, the detectability of local distributions of elevated *Sabellaria spinulosa* might be hampered.

The hull-mounted MBES provides higher positional accuracy and more consistent backscatter images compared to a towed SSS. In addition to backscatter, it also provides a bathymetric measurement. However, the horizontal mapping resolution of the MBES in the Brown Bank may be too limited to reliably distinguish the naturally occurring variation in the soil morphology from elevated patches of *Sabellaria.*

A multi-scale and multi-sensor mapping approach with the combination of a MBES, SSS, ROV video footage, and physical samples (e.g., box cores or Van–Veen grabs) is recommended for a full reef mapping campaign, as it was carried out in [1]. Such an approach provides the full picture of the *Sabellaria* reef habitat. The MBES provides detailed information about the seabed morphology and sediment distributions [15,16]. The MBES data can then be used to select suitable ground truth location for the ROV and grab sampling as well as to investigate preferred habitat characteristics of the targeted species. The SSS can be used for mapping the distribution of *Sabellaria* reefs, using the ROV video data to validate the interpretation of the SSS sonar data. Finally, the physical samples provide an accurate representation of the local seabed sediment characteristics and the reef biodiversity.

In this research, a unique multi-scale and multi-sensor data set was acquired in the Brown Bank, Dutch North Sea. The novelty of this paper is the application of a machine-learning algorithm to SSS data to semi-automatically map elevated *Sabellaria spinulosa* reefs in the Dutch Sea. This paper presents an overview of the Brown Bank area and describes the data-acquisition strategy. Next, the developed SSS data processing and classification workflow are described, resulting in maps of the estimated elevated *Sabellaria* reef presence. The quality of the results is discussed, and recommendations for future work are presented.

2. Materials and Methods

2.1. Study Area

The Brown Bank is located on the DCS, approximately 70 km west from the coastline, and measures roughly 70 × 30 km^2 (Figure 1a). The water depth ranges between 20 and 48 m (Lowest Astronomical Tide (LAT)), where the large variations are formed by the tidal ridges and swales crossing the area from the south to the north with a wavelength of 2 to 3 km. On top of these large-scale morphological bedforms, megaripples with a wavelength between 5 and 40 m and migrating with the main tidal current south-north, are present. The scientific expedition took place during 21 August and 1 September 2023. The large size of the Brown Bank and the limited time of 10 days yielded to the selection of four subareas (A, B, F, G) located in the swales of the tidal ridges (Figure 1b), since previous expeditions found *Sabellaria spinulosa* reefs in these regions [1,17].

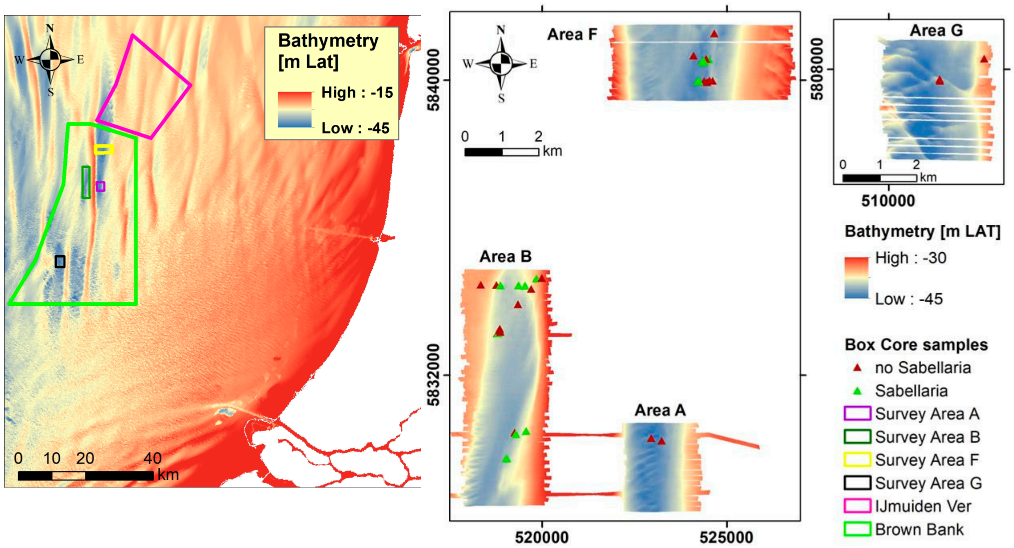

(**a**) (**b**)

Figure 1. (**a**) Bathymetric map showing the location of the Brown Bank in the North Sea; (**b**) Overview map of the northern Brown Bank showing the processed MBES bathymetric data and box core sample locations indicating the presence of *Sabellaria spinulosa* reefs. The Side Scan Sonar data overlaps with the bathymetric data. The coordinate system is WGS84 UTM 31N.

2.2. Data Acquistion

A multi-scale and multi-sensor approach was established to detect and map *Sabellaria spinulosa* reefs. The research expedition was carried out with the ARCA (IMO number 9167966), an 83 m long and 13 m wide vessel, which is used for surveying tasks, oil spill removal, and marine research. A hull-mounted Kongsberg EM 2040C dual-head MBES (Kongsberg Maritime Netherlands BV, Spijkenisse, The Netherlands) operating at 300 kHz and a towed Klein 5000 SSS (Klein Marine Systems, Salem, NH, USA) operating at 455 kHz were used to locate and map potential *Sabellaria* reef hotspots. The MBES was operated with a CW pulse, and the SSS was operated with a Chirp pulse. A CTD (Conductivity-Temperature-Density) probe was used to measure up two times per day the conductivity, temperature, and density of the full water column to compute the sound speed profile and the sound absorption.

A Saab Seaeye Panther-XT Plus ROV (Saab, Fareham, UK) equipped with a 4K resolution SUB-C camera was used for the visual identification and localisation of benthic species on the seabed.

A box corer with a diameter of 31.5 cm was used to retrieve physical samples from the seabed for grain size and biodiversity analysis. The vessel positioning was obtained with a

Septentrio AsteRx-U Fg GNSS receiver (Septentrio, Leuven, Belgium), with correction of Fugro Marinstar G4+ for PPP solutions. This yielded to a positioning accuracy of the MBES sonar head of a few centimetres. The ROV, SSS and box corer, being operated with a winch and cable, were equipped with a Kongsberg 501 USBL (Kongsberg Maritime Netherlands BV, Spijkenisse, The Netherlands) for positioning with respect to the vessel. The positioning accuracy of the USBL is expected to be around 1 to 2 m where the uncertainty increases with range.

The survey speed varied with current and wave direction between 4 and 7 km. The SSS ground range was fixed to 75 m. The tow fish flying height varied between 5 and 12 m, following roughly the recommendation of 10% of the ground range for *Sabellaria* mapping by [11]. The difficulty in keeping the tow fish flying height more constant was due to the strong variation in bathymetry and the manual operation of the winch. The survey speed and the ping rate, which both depend on the flying height and the fixed ground range, resulted in an along-track SSS sounding density between 30 and 50 cm. The SSS across-track resolution was significantly higher with 3 cm. The SSS settings resulted in a similar seabed coverage as the MBES (swath coverage-sector 130 degrees) for a water depth of 35 m. Test runs and previous experience showed that ensonifying the megaripples perpendicular to its crest orientation, i.e., survey lines with west-east and east-west direction, resulted in the best detectability of *Sabellaria* reefs [18]. The SSS data acquisition was carried out with SonarPro 14.1 (Klein Marine Systems, Salem, New Hampshire, USA) and the MBES data acquisition with QINSY 9.5.6 (QPS, Zeist, The Netherlands). MBES data processing was done with Qimera 2.5.4 and FMGT 7.10.3 (QPS, Zeist, The Netherlands).

2.3. Data Processing, Classification, and Mapping Workflow

A visual overview of the full data processing, classification, and mapping workflow is given in Figure 2. The data processing of the raw SSS data and the ROV video recordings defines module 1 as shown in the flow chart in Figure 2. The classification workflow runs from module 2 to step 6, whereas the mapping and generation of the final maps is conducted in module 7.

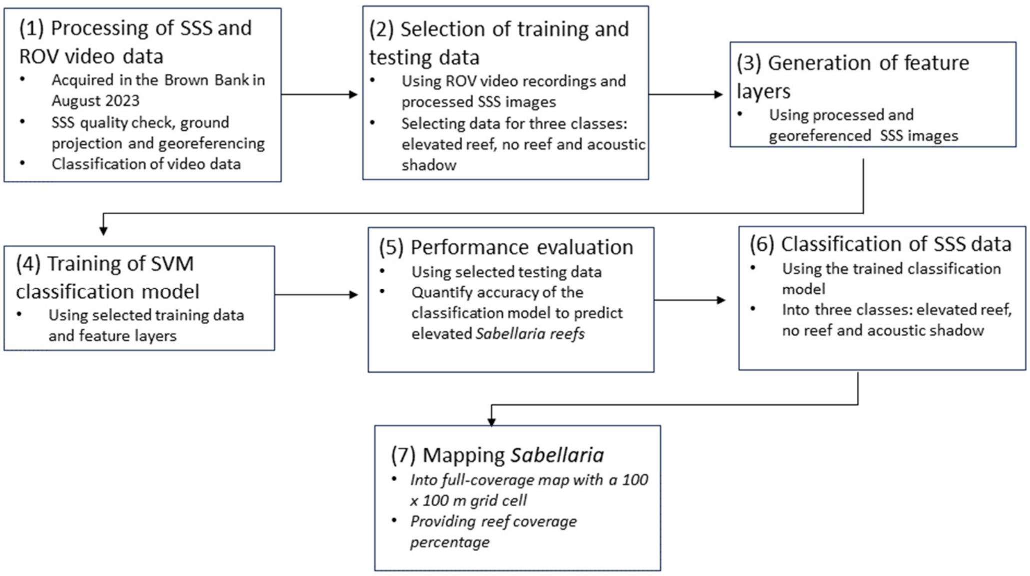

Figure 2. Overview of developed data processing and classification workflow to map *Sabellaria spinulosa* reefs.

The MBES bathymetry was used in the classification workflow to improve the geographic overlap between the SSS and ROV data enabling a more accurate selection of training and testing data.

2.3.1. Side Scan Sonar Pre-Processing

The processing of the SSS data was carried out in MATLAB R2022b (Module 1, Figure 2). Therefore, the raw SSS data was first extracted from the Klein sonar SDF file format and saved to the MATLAB MAT file format. First, the data was detrended along the slant range dimension to remove the range decay caused by sound absorption and the angular backscatter variability. This was done by computing the 75th percentile of the amplitude range curve (also called amplitude time series) over consecutive adjacent 3000 pings. This curve was then subtracted from each ping to detrend the data. Furthermore, poor-quality data close to the nadir (specular noise at high incident angle reflections, 0 to 25 degrees) and pings where the ship was turning were discarded. The positioning of the tow fish was based on layback correction using the cable length for the first week SSS data set. For the second week data set the positioning of the tow fish was obtained from the USBL signal (The USBL was only available in the second week). The manual winch operating mode with a cable length of up to 100 m and a sailing direction perpendicular to the currents resulted in a high tow fish position uncertainty, whereas the USBL positioning uncertainty was estimated to be around max 2 m. The sailing direction was chosen to be parallel to the megaripple crest, as it was considered as favourable for reef detection. In combination with uncertainties in the ground projection due to heading sensor uncertainties, sound speed variation (constant sound speed is assumed) and varying morphology (flat seabed is assumed), a maximum cumulative positioning error of 30 m for SSS images of the first week was observed. Using the USBL for the tow fish positioning yielded to good positioning of the tow fish and significantly improved positioning of the SSS image with a maximum positioning error estimated at 10 m. The positioning offset were estimated using recognizable features in the MBES bathymetry data.

In the last step the sonar time series is projected on a regular $10 \times 10\ \text{cm}^2$ georeferenced grid in WGS84 UTM 31N coordinates, generating for each track line a georeferenced SSS image. The similarity of the sonar images varied throughout the data set due strong variation of the two-fish altitude (5 to 12 m) and varying morphology.

2.3.2. ROV Video Recordings

The video recordings were analysed into 10 classes: sand, sand with low, medium and high shell coverage, and flat reef as well as elevated reef with low, medium, and high coverage (Module 1, Figure 2). Low shell and reef coverage means < 20% (including individual clumps of *Sabellaria spinulosa*), medium is between 20% and 50% and high > 50% seabed coverage. The flat reef class comprises *Sabellaria* with an elevation of <5 cm and the elevated reef class defines elevation of 5 cm to 20 cm. The classification for *Sabellaria* reefs is based and modified from categories proposed by Gubbay [19].

The time stamp and geographical coordinates of every transition between classes were reported. In postprocessing the coordinates and the class number were linearly interpolated on 5 s intervals. Examples of optical ROV images, including the class labelling, are shown in Figure 3. An example of a classified video track into the 10 classes is shown in Figure 4. Because of low sensitivity of the SSS to flat *Sabellaria* reef patches and the main interest in elevated reefs, the 10 classes were reduced into two classes for the SSS classification: (i) elevated reefs and (ii) no reef (see Figure 4). An additional third class the (iii) acoustic shadow zones was added (see Figure 4). This class defines the area where the acoustic signal is blocked and is required for the final estimation of the reef coverage. The no-reef class category contains the original seven sand and flat-reef classes. The elevated-reef category contains the three elevated (low, medium, and high coverage) reef classes.

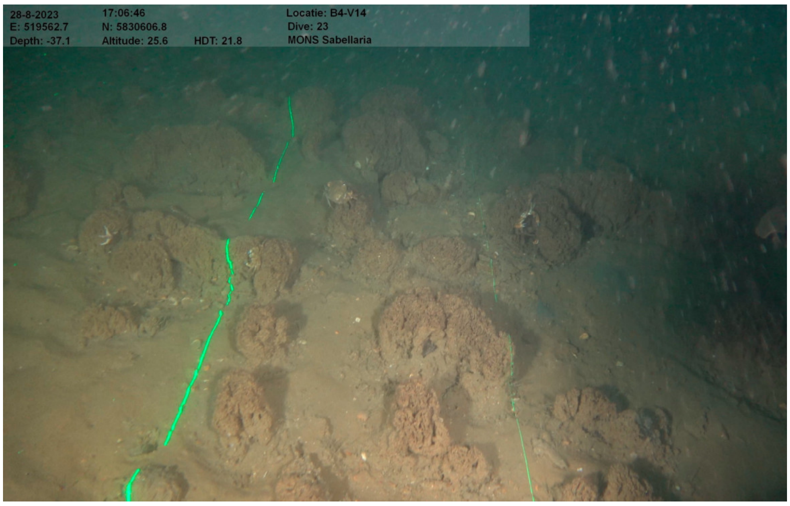

(**a**)

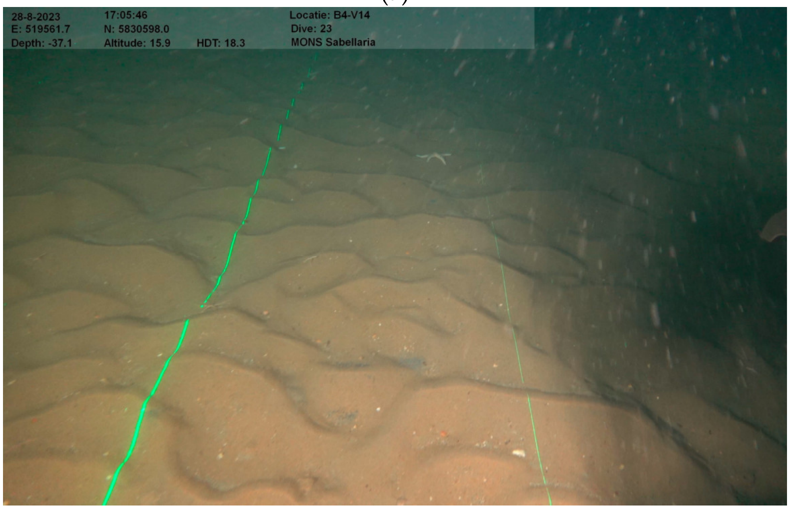

(**b**)

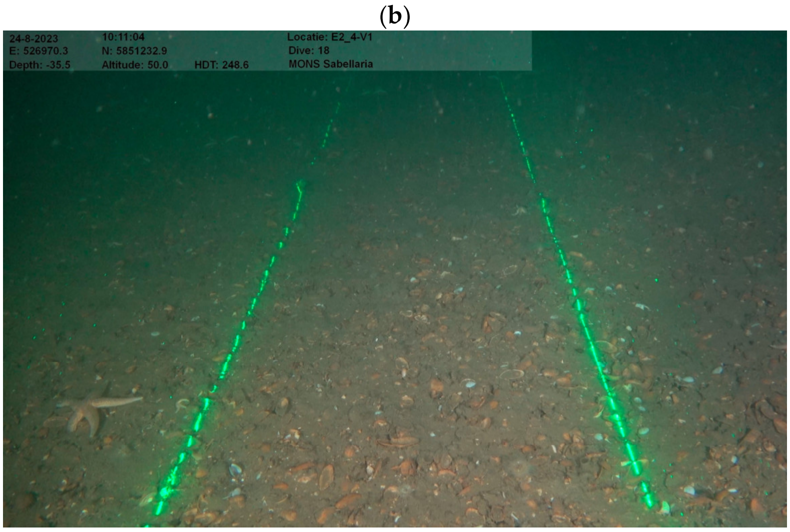

(**c**)

Figure 3. ROV video footage (**a**) high coverage, elevated *Sabellaria spinulosa* reefs labelled as "elevated reef", (**b**) sand and fine-scale sand ripples labelled as "no reef", and (**c**) sand with high shell coverage labelled as "no reef". The green lines originate from the ROV laser indicating a distance of 50 cm, which is used as an estimate for object dimensions.

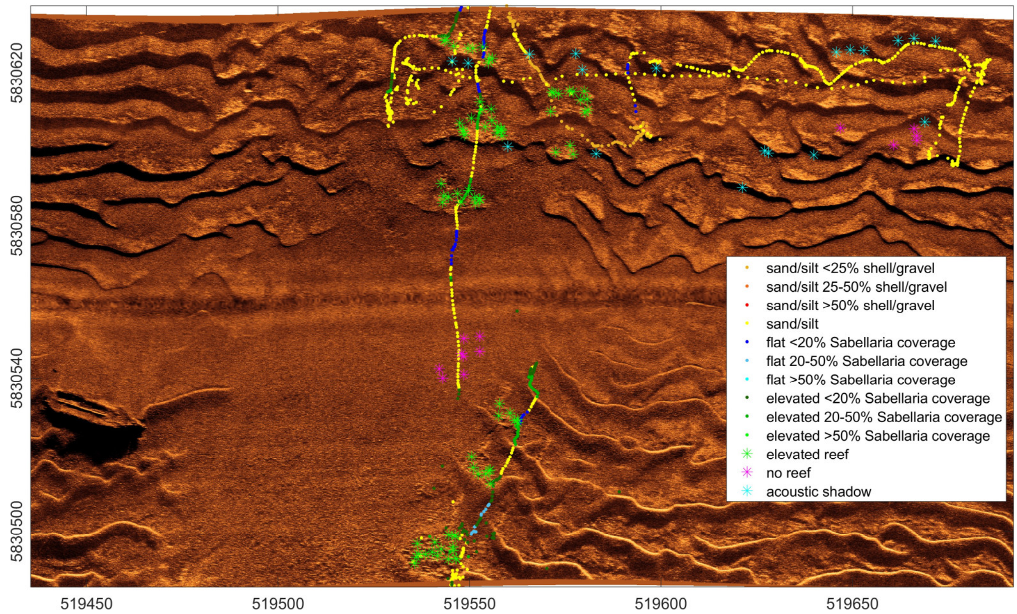

Figure 4. Processed and georeferenced SSS image with classified video tracks (dots) and selected training samples (asterisk) considering the geographical offset between ROV and SSS data. The coordinate system is WGS84 UTM 31N.

2.3.3. Classification Workflow

A variety of machine learning algorithms, the support vector machine (SVM), decision tree, neural network, naïve Bayes, and k-nearest neighbour (k-NN), were tested. Based on the performance analysis (see Section 3.1), the SVM was chosen for the final classification of the SSS data [20]. The SVM is a supervised classification method that is a subcategory of machine learning or Artificial Intelligence (AI). A supervised classification method uses features layers, also called input layers (here, the acoustic image and its derivatives) and a pre-defined number of classes (here, elevated reef, no reef, and acoustic shadow) to train a model. For training and evaluating the model, training and testing data needs to be selected on locations where the feature layers are available and the true class is known. The trained model can then predict the predefined classes for every location at which the feature layers are available. Feature layers, fed into the machine learning algorithm, are generated using the pre-processed SSS images. A normalisation of the feature layers was required for the SVM (opposed to a decision tree) to avoid dominance of features with high values.

2.3.4. Training and Testing Data

A variable geographical offset between SSS data and ROV video recordings hampered the automatization of the selection of the training and testing data. Therefore, the training and testing data was selected manually in the areas where labelled ROV video data was available and data could be selected manually with a sufficiently high (expert assessment) confidence (Module 2, Figure 2). Since only a limited amount of training data was available, manual labelling of areas outside (but nearby and with similar acoustic pattern) the ROV track was needed to obtain enough training and testing data. The same features visible in the MBES bathymetry and SSS images were used to determine the offset and to geographically shift the SSS images to the correct position (using the MBES position as ground truth). The labelling of the training and testing data was based on the three classes (i) elevated reef, (ii) no reef, and (iii) acoustic shadow. The same SSS track line was not used for training and testing the classifier to reduce the risk of overtraining the classifier. In total, 3707 training and 2477 testing samples were manually selected. The number of training/testing samples per class is not fully balanced with 717/222, 1735/1478, and 1255/777 samples for the reef, no reef, and acoustics shadow class. The training data set was prioritized to maximize the reef samples for the training. Therefore, the training data set is better balanced than the testing data set. Examples of a classified video track line on top of the SSS image and the corresponding manually selected training data are shown in Figure 4.

2.3.5. Feature Input Layers

Two well-known feature-generation methods, the Gabor filter and the Gray level Co-occurrence Matrix (GLCM) metrics, were employed (Module 3, Figure 2). Bianconi et al. [13] has shown that the Gabor filter is an effective method to identify textures in the side-scan sonar image characteristic for *Sabellaria spinulosa* reefs. The GLCM performance was lower in this study, but it was successfully employed in other studies (e.g., [21]).

Gabor filter [1] is applied to obtain directional spatial wavelength information. This filter investigates a specific spatial frequency (i.e., wavelength) content in the image in specific directions in a localized region around the point or region of analysis. A variety of different wavelengths (0.5, 0.8, 1.0, 1.5, and 2.0 m) towards the direction of 30 (SSW-NNE), 45 (SW-NE), 90 (W-E), and 135 (NW-SE) degrees were analysed.

Gray level Co-occurrence Matrix [2] (GLCM) metrics contain information about the texture in the image similar to the Gabor filter. Texture with different spatial information can be highlighted by computing the GLCM for different pixel distances (i.e., a pixel pair) in the image. Features were created for pixel pairs of 1 and 5 pixels (i.e., 0.1 and 0.5 m distance between adjacent pixels) for a bounding box of 1×1 m^2 and 2.5×2.5 m^2. Hence, containing 100 and 625 SSS samples per box, given the 10×10 cm^2 resolution of the gridded data. This way, patterns with different spatial scales are highlighted. From the GLCM, various statistical texture metrics that consider the spatial relationship can be computed. This involves the following four features:

Contrast: Measures the local variations in the GLCM.

Correlation: Measures the joint probability occurrence of the specified pixel pairs.

Energy: Provides the sum of squared elements in the GLCM. Also known as uniformity or the angular second moment.

Homogeneity: Measures the closeness of the distribution of elements in the GLCM to the GLCM diagonal.

In addition to the features layer computed with the Gabor filter and GLCM, which can be considered as second-order texture analysis [22], first-order textures as the mean and standard deviation (STDV) of the signal amplitude (in dB) as well as the ground range were additionally created. The values were computed for the same bounding boxes as used for the GLCM layers.

Using the different settings for the feature-generation methods, a total of 36 feature layers were generated, which can serve as an input for the machine learning classifiers. The 36 feature layers were combined in different variations to investigate an optimal combination of feature layers with respect to prediction accuracy and computation efficiency. In addition, a principal component analysis (PCA) was applied to the feature layers to investigate the usage of the data reduction. This led to the selection of 25 different combinations of feature layers, further called simulation runs (see Appendix A).

2.3.6. Support Vector Machine (SVM) Classifier

The general concept of SVM is to maximize a hyperplane where the hyperplane is a separator between two classes. A hyperplane between two classes can be found by measuring the margin of the hyperplanes and finding its maximum. The margin is the distance between the hyperplane and the closest data from each class [23]. The closest data is called the support vector, which are used to classify the data into the pre-defined classes. The hyperplanes are found by transforming the original feature layers into higher-dimensional space where the classes are easier to separate via a kernel function. For this study the MATLAB (version R2022b) implementation of the SVM was used. The Kernel function can be linear or non-linear (e.g., Gaussian Kernel function) and can be chosen as a setting of the classifier in the MATLAB implementation. Similar performance was achieved for the linear and Gaussian Kernel function. To avoid further complexity of the algorithm, the linear Kernel function was chosen. The parameter controlling the data fit, called BoxConstraint in MATLAB, was set to a low to intermediate value of 1. A low value (e.g., 0.1) increases the margin, and the SVM becomes less sensitive to noise but possibly allows more misclassification. A high value (e.g., 100) decreases the margin, and the SVM becomes more sensitive to the training data, trying to reduce misclassification, which could result in overfitting, in particular when the data is noisy. Other hyperparameters were automatically optimized for this data set by the MATLAB implementation.

The classifier was trained on the training sample data set with 3707 samples selected from area A, B, F, and G (Module 4, Figure 2). The evaluation of the performance of the classifiers was carried out on the test data set with 2478 samples selected from the same areas A, B, F, and G (Module 5, Figure 2). Here, a sample corresponds to a 10×10 cm^2 grid cell for which the true class and the feature values are known. Both the training and testing samples were selected following the procedure described in the previous section. The test data set was used to compute the confusion matrix from which the following important evaluation parameters can be obtained:

- the true positive rate (Sensitivity) and false negative rate, which summarize how well the true class is predicted correctly of falsely.
- the true positive predictive rate (Precision) explains how well the prediction corresponds to the true class.
- The overall accuracy is the indicator how well all classes combined are correctly predicted.

The trained linear SVM classifier was then applied to each sonar track line separately to classify the data into the three classes: (1) elevated reef, (2) no reef, and (3) acoustic shadow (Module 6, Figure 2).

2.3.7. Mapping

Next, the classified SSS lines were used to compute maps of the *Sabellaria* reef percentage coverage (Module 7, Figure 2). Because of the positioning uncertainty of the sonar data, the removal of the nadir region and not always full overlap of the track lines, the data of different sonar tracks at 10×10 cm^2 resolution were aggregated onto a larger 100×100 m^2 grid, counting the 10×10 cm^2 gridded data that was labelled as reef or non-reef (discarding pixels with the acoustic shadow label). This procedure yields to a map displaying the coverage of the seabed with elevated *Sabelleria* reefs in percent.

3. Results

3.1. Performance Analysis

For the performance analysis the precision and sensitivity of the SVM classifier trained on 24 different sets of feature layers were computed from the testing data set (Figure 5). The used feature layers per simulation run are listed in the Appendix A. It should be noted that the overall accuracy tends to be biased towards the precision and sensitivity of the no-reef and acoustic shadow class due to the unbalanced testing data set with only 222 out of 1777 samples belonging to the reef class. The results show that about 20 from the original 36 feature layers are sufficient to achieve good performance (e.g., simulation run two or three). However, a combination of the Gabor filter, GLCM, and the basic statics (first-order derivatives) appears to be required to achieve good performance for every class. For example, if only the Gabor filter is used as in simulation 10, 11, 12, the reef and no-reef class are almost equally well-predicted compared to the other simulations, but the SVM classifier struggles to predict the acoustic shadow class. Using only the first-order derivatives (simulation 5, 6, and 7), the classifier performs very poorly for the reef class. A data reduction via a PCA, either applied to all feature layers (simulation 18, 19, 20) or just to the features obtained from the Gabor filter (simulation 13 and 14), decreases the performance over all classes. Using only a single wavelength and orientation in the Gabor filter (simulation 24) also reduces the performance. The tile size for the GLCM, the exact wavelength and orientation for the Gabor filter, or the use of the ground range (e.g., simulation 1, 2, 3, 4, 15, 16, 17, 21, 22, 23), seems, however, less important and does not affect the performance significantly. For the generation of the classification results and the elevated *Sabellaria* reef presence map, simulation run two with an overall accuracy of 0.89, a precision of 0.49, and a sensitivity of 0.52 for the reef class was chosen. This feature combination set has a good trade-off between high computational speed and good performance and was therefore selected in this study.

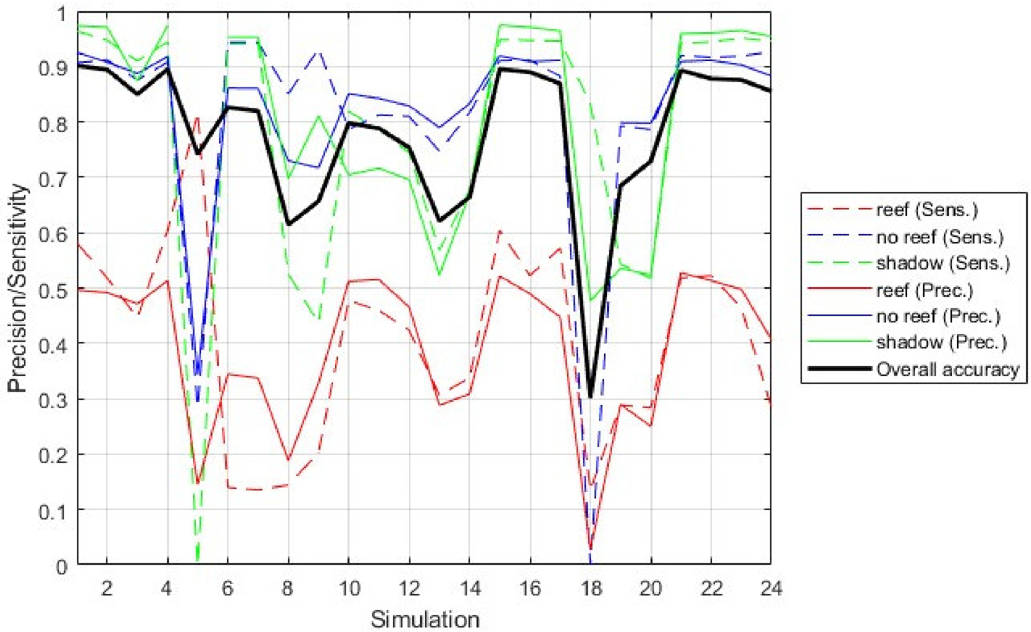

Figure 5. Performance analysis showing the sensitivity (Sens.) and precision (Prec.) of the SVM classifier trained on 24 different feature layer combinations.

Other classifiers, such as the decision tree, neural network, naïve Bayes, and k-NN, were tested as well. Even though the sensitivity of the reef class is lowest for the SVM, it shows the best performance in terms of the precision of the reef class and the total accuracy (Table 1). The precision was rated as more important, since it provides an estimate how often the predicted reef is a true reef and therefore more suitable for unbalanced testing data sets. This gives an indication of how trustworthy or uncertain the reef prediction is. The classifiers are available in the MATLAB modelling environment (part of the machine learning toolbox) and were executed with default MATLAB settings. A detailed performance analysis of different classifiers was not in the scope of this research. Therefore, the description of the methodology and the results were focussed on the SVM classifier.

Table 1. Performance analysis of different machine learning algorithms for simulation run two. The sensitivity and precision are given for the reef class.

Algorithm	Sensitivity	Precision	Overall Accuracy
Decision Tree	0.60	0.40	0.86
Neural Network	0.61	0.45	0.88
Naïve Bayes	0.55	0.46	0.84
K-NN	0.59	0.38	0.84
SVM	0.52	0.49	0.89

Figure 6 shows a subset of an SSS image and the corresponding classification results obtained from the trained SVM classifier. In the SSS images the testing samples, obtained from the manual selection of the ROV video recordings, are plotted on top. In the classified images the positive (green) or false (red) detection of the given samples are plotted on top. In these examples, all testing samples of the acoustic shadow and no reef class are correctly predicted, as it was expected from the performance analysis showing high-sensitivity values for these classes (Figure 5). Approximately half of the elevated reef class samples are correctly predicted in this example.

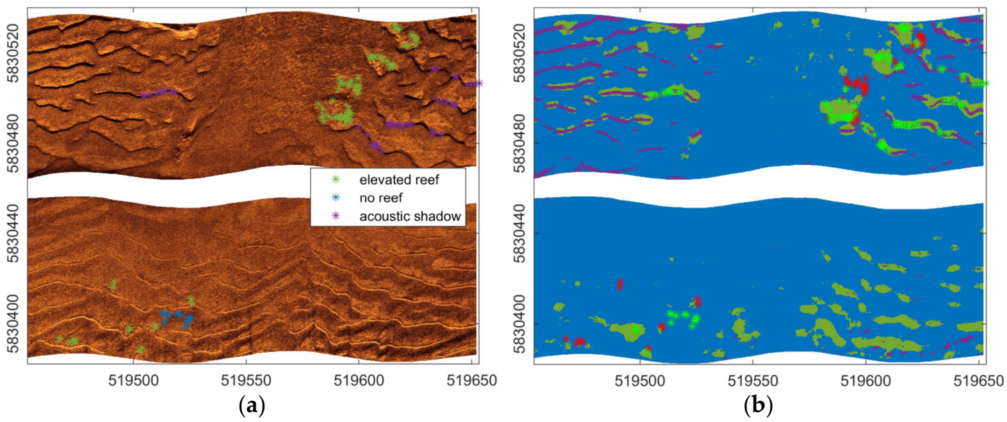

Figure 6. Example SSS line for validation of the trained SVM model using the testing sample data set. (**a**) SSS image with testing samples for validation indicated by asterisks. (**b**) Classification into elevated *Sabellaria spinulosa* reef (green), no reef (blue), and acoustic shadow (purple) with indication of true (green asterisks) and false (red asterisks) detections. The coordinate system is WGS84 UTM 31N.

3.2. Classification

The SVM classifier was applied per ground-projected sonar track line individually, and thus the classification is not influenced by the positioning uncertainty of the SSS data. Merging the classified SSS track lines into a full-coverage map was carried out afterwards in light of the high positional uncertainty of the data in the first week. Figure 7 shows two examples of the classified SSS track lines acquired in area B and F. While the track line in area F has only a small percentage of 0.6% of the seabed classified as elevated reef, the track line from Area B has a higher percentage of reef coverage with 15.4%. For the computation of the seabed reef coverage in percent, the acoustic shadow class is discarded. The classified SSS images, in particular the line from area B, shows visually that the elevated *Sabellaria* reefs tend to be located on the northside of the megaripples. The deepest part of the trough is located in the blind zone of the sonar (acoustic shadow), but in general, the *Sabellaria* reefs decreases towards the crest, being in alignment with the video recordings, which have shown higher *Sabellaria* reefs presence in the trough and the absence of *Sabellaria* reefs on the crest.

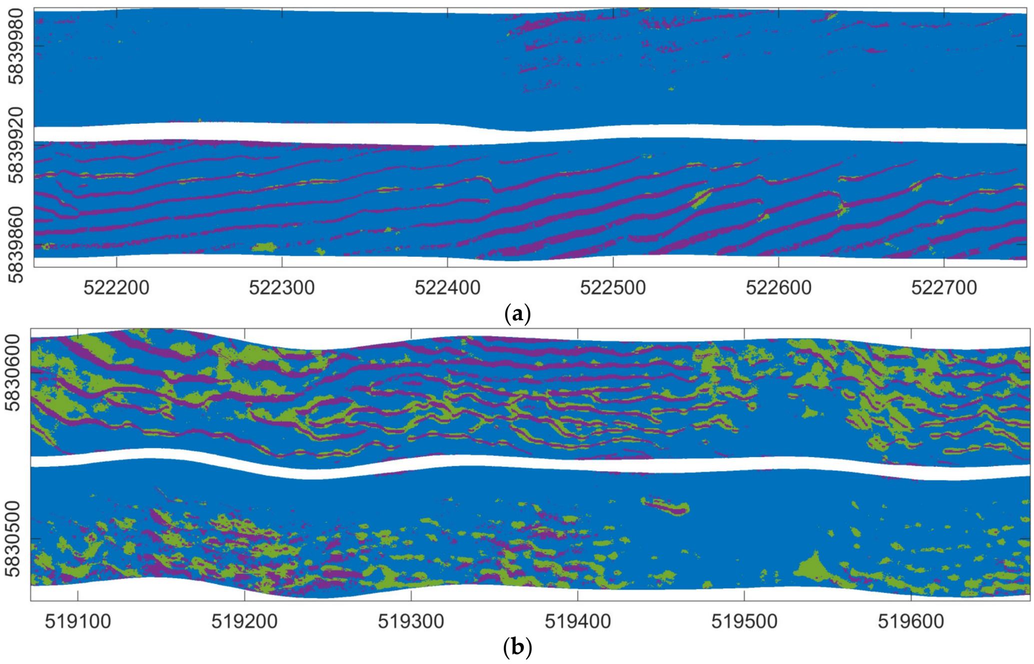

Figure 7. Classified SSS track lines with three classes: elevated reef (green), no reef (blue) and acoustic shadow (purple). (**a**) SSS line from area F with low reef coverage of 0.6% and (**b**) SSS line from area B with high reef coverage of 15.4% around a *Sabellaria spinulosa* reef hotspot. The coordinate system is WGS84 UTM 31N.

Analysis of the classified SSS results showed that below 30 m ground range from the nadir there was a drop on the predicted amount of *Sabellaria* reefs, suggesting that the classifier was not sufficiently trained in this region. Most likely, the low incident angle at this region reduces the detectability of the small-scale relief of the reefs. This also intuitively leads to fewer training samples being selected between 0 and 30 m ground range. Therefore, the classifier appeared to be less well-trained at short ranges and is therefore likely to underpredict the presence of reefs. The removal of the data below 30 m ground range resulted in data gaps when using a 50×50 m^2 grid cell, which would already account for the positional uncertainty of 30 m. Since the small-scale information is already removed with 50×50 m^2 grid cell, a 100×100 m^2 grid cells was used to compute a reliable assessment of the *Sabellaria* reefs percentage coverage. This yielded to a full-coverage *Sabellaria* reef presence map without data gaps for area A, B, F, and G.

Finally, the estimated reef coverage is multiplied with the precision (true positive prediction rate) of 0.49 (49%) of the classifier to account for the uncertainty in the prediction. Table 2 shows the percentage of reef coverage for the four considered areas with values between 3.8 and 5.7%.

Table 2. *Sabellaria spinulosa* reef percentage coverage and area estimates using the developed classifier.

Area ID	Area Size (Percentage Coverage)
Area A	0.24 km^2 (5.7%)
Area B	0.78 km^2 (4.8%)
Area F	0.39 km^2 (4.1%)
Area G	0.37 km^2 (3.8%)

The generated *Sabellaria* reef presence maps in combination with the MBES bathymetry maps allow to interpret the large-scale distribution of *Sabellaria* in the Brown Bank environment (Figures 8 and 9). The surveyed areas A, B, F, and G cover all from west to east the swale between the tidal ridges. The highest *Sabellaria* reef percentage is mostly located to the east of the deepest location of the swale, indicating a preference of *Sabellaria spinulosa* for settlement. This is visually shown in Figures 8 and 9 for Area B and F, respectively (The maps for Area A and G can be found in the public data set [24,25]). The location and spatial orientation of the highest settlement density of *Sabellaria* in area B, detected by the classifier, matches very well with the manual interpretation of the SSS image by an expert (Figure 8).

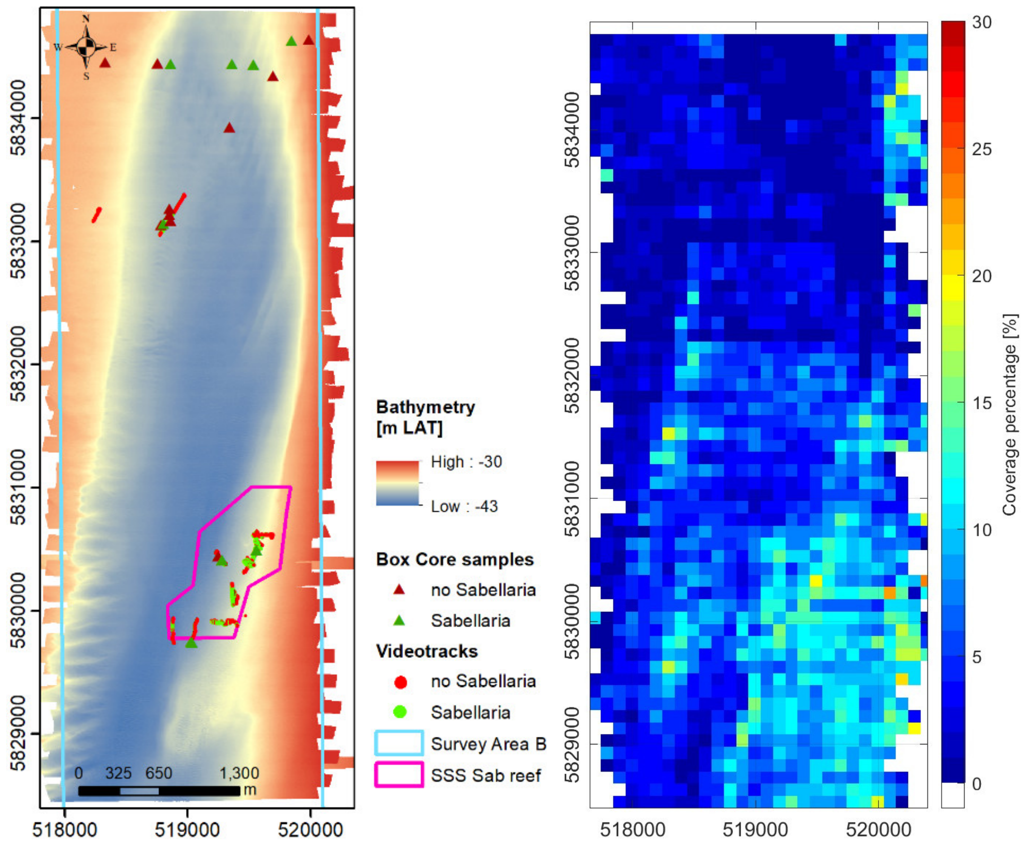

(**a**) (**b**)

Figure 8. (**a**) MBES bathymetry of Area B. Box cores and video tracks indicating the absence and presence of *Sabellaria spinulosa* reefs (No distinction between flat and elevated *Sabellaria* reefs is made). The pink polygon shows the manually mapped area where a blotchy pattern in SSS imagery indicates the presence of elevated *Sabellaria* reefs. (**b**) *Sabellaria* reef presence map for area B. Total coverage of the seabed with elevated *Sabellaria* reefs is 4.8%. The cell size is 100×100 m^2. The coordinate system is WGS84 UTM 31N.

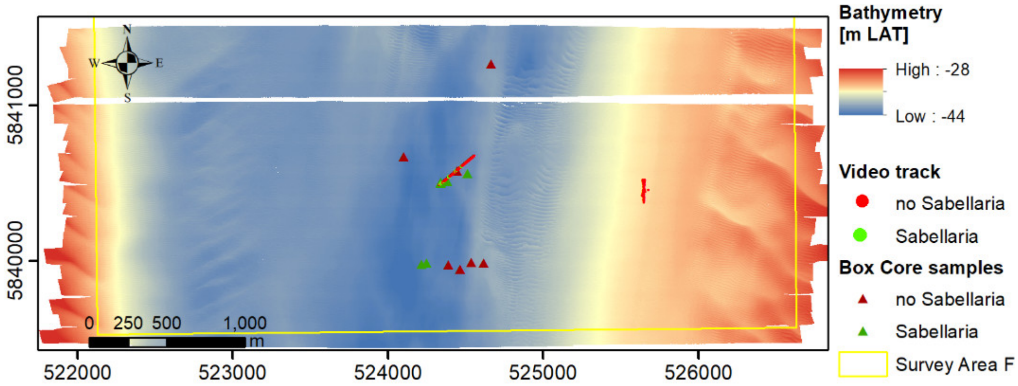

(**a**)

Figure 9. *Cont.*

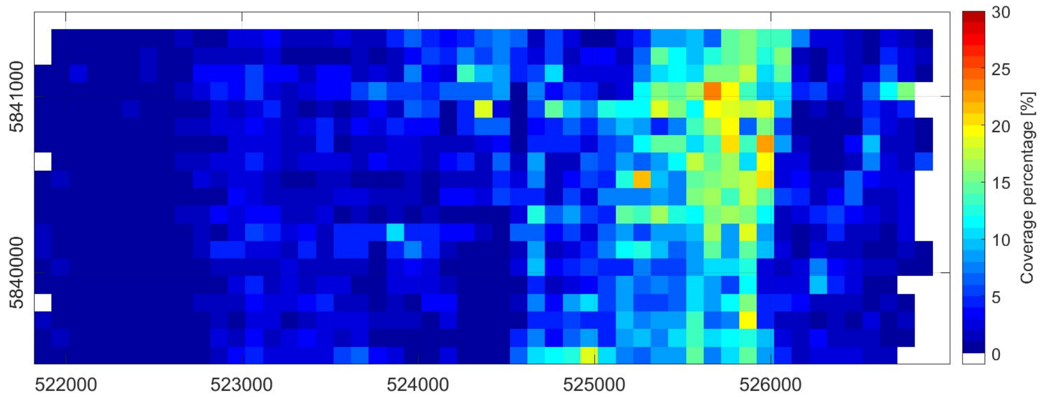

(**b**)

Figure 9. (**a**) MBES bathymetry of Area F. Box cores and video tracks indicating the absence and presence of *Sabellaria spinulosa* reefs (No distinction between flat and elevated *Sabellaria* reefs is made). (**b**) *Sabellaria* reef presence map for area F. Total coverage of the seabed with elevated *Sabellaria* reefs is 4.1%. The cell size is 100 × 100 m^2. The coordinates are in WGS84 UTM 31N.

4. Discussion

The expedition to the Brown Bank in 2023 to detect and map *Sabellaria spinulosa* reefs was driven by a first discovery of *Sabellaria* reefs in 2017 by Van der Reijden et al. [1]. They detected *Sabellaria* reefs with ROV video footage and used a MBES for selecting promising areas for ground truthing. In the expedition in 2023, the presence of the majority of the previously detected *Sabellaria* spots in 2017 could be confirmed via ground truthing and SSS data. Using the SSS data, this paper presents for the first time a semi-automated SSS classification workflow for mapping *Sabellaria* reefs in complex environmental conditions typical for the North Sea (i.e., deep water, strong bathymetric variations with varies morphological patterns, moderate tidal currents). The generated *Sabellaria* reef presence maps and the estimated percentage of reef coverage will be of great use for ecologists [26], the offshore industry or governmental organisations [4]. Based on the generated maps, researchers can further investigate and plan new studies for this species and decision-makers can make better informed decisions on nature-restorative measures in the northern Brown Bank.

The developed SSS processing workflow is adaptable to other environmental areas and potentially applicable to classify other reef types and habitats. Clearly, training and testing new classifiers with sample data sets from such new environments and SSS configurations are indispensable for validated predictions. Preliminary investigation into the differences in performances among the areas [25] showed that the best performance was obtained in the area with the most training samples (Area B). Augmentation techniques could be used to increase the number of training and testing samples for the reef class, generating a more balanced data set.

The overall accuracy of the SVM classifier with values around 0.9 (90%) was relatively good. For example, Febriawan et al. [22] used a linear SVM applied to SSS data for habitat classification and achieved an overall accuracy of 0.77. However, the precision and sensitivity with values of around 0.5 for the elevated reef class could be considered as low, e.g., compared to the study by Bianconi et al. [13], who obtained a "*Sabellaria* accuracy" (probably comparable to the sensitivity) of around 0.9 using a nearest-neighbour classifier in combination with a Gabor filter. The comparison of the classifier accuracy across studies is only an indication as the data quality and environmental complexity are observed to vary among the different studies. In the application of machine learning to SSS data for habitat classification, multiple factors can influence the classification accuracy. The data quality is of particular importance, which depends on the hardware, software, survey strategy, and the environment. In this expedition, the positional stability (i.e., varying flying height, lateral movements, and crabbing) and positioning accuracy of the tow fish was relatively low. In particular, the presence of *Sabellaria* between the megaripples hampered the detectability. The slope of the megaripples blocks part of the sonar signal and also increases the reflectivity. This, in combination with the accumulation of shell fragments, which can also cause a blotchy acoustic pattern, hampered the classification compared to an area where *Sabellaria* reef is located on a flat and homogenous sediment. How well the *Sabellaria* reefs are developed also affect the detectability. Individual clumps are more difficult to detect than well-developed and extended reefs, as, for example, shown for the southern North Sea in the Norfolk Sandbank and Saturn reef [12].

Potential improvements for detectability could be achieved by slower vessel speed increasing the along-track sounding density and a higher sonar frequency increasing the across-track resolution. Obtaining a stable fish position could be achieved by using an Autonomous Underwater Vehicle (AUV). The AUV could also be equipped with a video camera, which could increase the size of the training and testing data set for the classifier. Perhaps, a distinction between the reef coverage (low, medium, and high) or the flat *Sabellaria* (elevation < 5 cm) could be achieved with these improvements.

Feature layers were created from the raw data (here, the pre-processed SSS line) in order to create a more effective set of inputs for the machine learning algorithm. It helps the algorithm to better predict the classes (i.e., the *Sabellaria* reefs). The developed classification workflow is considered as a traditional approach according to the literature of SSS classification [9]. The feature layers were generated with manually selected texture analysis methods (Gabor filter and GLCM), and the SVM was used for classification. The rationale behind using a traditional or feature layer approach (opposed to just feeding in raw data and letting a deep learning algorithm determine the feature layers [9]) was that (i) satisfactory results were obtained using the tested feature layers in literature [13,21], (ii) enforcing a limited set of feature layers reduces the risk of overtraining on non-relevant features when only a limited set of training and test data is available [27], and (iii) it allows selection of feature layers based on acoustical and morphological domain knowledge as well as on information about reef dimensions and shapes. For example, the settings for creating the different feature layers from the acoustic SSS image can be chosen in correspondence with the targeted environment like wavelength of megaripples or height and size of the reefs. In [9], a review of the upcoming field of deep learning-based computer vision methods for sonar imagery is given. They list a few promising studies that used deep learning for the calculation of abstract features for object and mine detection (e.g., [28,29]). One study also used deep learning for reef mapping [30]. However, the type of reef is not stated in the publication, but it should be further investigated how the deep learning classifiers would perform on *Sabellaria spinulosa* reefs.

The low positioning accuracy of the first-week data set due to missing USBL locator did not allow an aggregation of the first- and second-week data sets onto a finer (<10 m) grid. A workaround was the aggregation of the classified pixels on a larger grid cell of 100×100 m^2 and the computation of the reef percentage per grid cell. This procedure allowed to obtain a full-coverage map and to cover the large nadir gap, but it hampered the use of the classification results for a habitat analysis via a correlation with local morphological features derived from the MBES measurements. With a USBL locator (second week), the position of the tow fish (w.r.t. the vessel) could be measured with an accuracy estimated at max 2 m. However, beside the uncertainty in the positioning of the tow fish, several additional factors (e.g., heading sensor uncertainty, sound speed variation, deviation from the flat seabed) contribute to the total positioning uncertainty of the georeferenced sonar image as well. Therefore, maximum positioning offsets of 10 m were still observed for the second-week data set. Since all factors vary while sailing, the positioning uncertainty varies throughout the data sets. For the selection of the training and testing data set, the MBES bathymetry has been used for manually aligning the SSS images with the ROV tracks using features visible in both data sets. Zhang et al. [31] used the similarity of MBES bathymetry and SSS image (backscatter) contours to carry out an automized matching and superposition. However, matching 3D MBES terrain and 2D SSS reflectivity images is difficult, and the methods were ineffective in seabed with varying morphology with a single sediment (like the megaripples in the Brown Bank) or a flat seabed with various sediments. Zhao et al. [32] developed a matching method based on MBES and SSS backscatter images making use of the same physical measurement principle, which visualizes seabed texture and sediment variation in a similar way. This could be a promising algorithm to improve the positioning accuracy of the SSS data acquired in this study and eventually to use the classification results for further habitat analysis.

5. Conclusions

Sabellaria spinulosa reefs were successfully detected and mapped in parts of the northern Brown Bank, the Netherlands. The application of the side-scan sonar (SSS) was successful to identify elevated *Sabellaria* reefs on the seabed. In the video footages, acquired with a remote operating vehicle (ROV), individual to densely populated clumps of flat (<5 cm elevation) and elevated (5 to 20 cm elevation) *Sabellaria* were detected. A machine learning classification workflow was developed to semi-automatically map elevated *Sabellaria* reefs employing the acquired SSS data set and ROV video recordings. The developed classification model, based on the support vector machine (SVM) classifier, mapped the elevated *Sabellaria* reefs with a precision (true positive prediction rate) and sensitivity (true positive rate) of 0.52 (52%) and 0.49 (49%), respectively. This approach resulted in estimated reef coverage percentages between 3.8 and 5.7% for the different areas, which were located in the swale between the tidal ridges of the Brown Bank.

The reef presence maps could be used for large-scale interpretation of the spatial patterns of *Sabellaria* reefs, indicating a preference of *Sabellaria spinulosa* for settlement to the east of the deepest part of the swale between the tidal ridges. A visual inspection of the high-resolution (10×10 cm^2) SSS classification maps, confirmed by the ROV video recordings, indicated the preference of *Sabellaria spinulosa* for settlement in the troughs towards the stoss side of the megaripples.

Low positioning accuracy and limited usable ground range of the SSS data set hampered (1) the generation of the final *Sabellaria* reef presence maps with a higher resolution than the obtained 100×100 m^2, (2) the fine-scale comparison (meter scale) with the multibeam echosounder (MBES) data for a statistical habitat analysis, and (3) the integration of the MBES data into the classification workflow due to the positional mismatch between the SSS and MBES data. Automated matching and superposition methods employing the MBES and SSS data could increase the positioning confidence of the SSS images and consequently extent the use of the classification maps.

Author Contributions: Conceptualization, T.C.G. and B.B.; Methodology, T.C.G. and B.B.; Software, T.C.G. and B.B.; Validation, T.C.G. and B.B.; Formal analysis, T.C.G.; Investigation, T.C.G., B.B., and O.B.; Resources, T.C.G. and B.B.; Data curation, T.C.G.; Writing—original draft preparation, T.C.G.; Writing—review and editing, B.B. and O.B.; Visualization, T.C.G. and B.B.; Supervision, T.C.G. and B.B.; Project administration, B.B. and T.C.G.; Funding acquisition, B.B. All authors have read and agreed to the published version of the manuscript.

Funding: The research was funded by the European Maritime, Fisheries and Aquaculture Fund (EMFAF) of the European Union.

Institutional Review Board Statement: Not applicable.

Informed Consent Statement: Not applicable.

Data Availability Statement: The raw and processed data is publicly available via the Marine Information and Data Centre (IHM) by Witteveen and Bos [24]. The developed software (side-scan classification workflow including module 3 to 7, see Figure 2) is made available on the WOZEP GIT repository (https://wozep.nl/git/MONS/04_benthos_and_habitats/-/tree/main/sabellaria_reefs, accessed on 1 November 2024).

Acknowledgments: This research was made possible by the MONS (Monitoring en Onderzoek Natuurversterking en Soortenbescherming) program led by Rijkswaterstaat.. Special thanks go to the crew of the ARCA of Rijkswaterstaat for their supporting role in acquiring the acoustic and ground truth data. Furthermore, thanks to Eurofins Aquasense and Waardenburg Ecology for analyzing the ground truth data.

Conflicts of Interest: The authors declare no conflict of interest.

Appendix A

Table A1. Description of features layers used in the simulation runs. Amp is the median SSS amplitude computed over the given tile size, STD is the standard deviation of the SSS amplitude computed over the given tile size, and GR is the ground range or also called distance from nadir. All in the GLCM column means that all four GLCM layers are computed for the given tile size and pixel pairs. All in the Gabor column means that all layers for the given wavelengths and angles are computed, while PC means that the principal components were computed from the given wavelengths and angles.

Run	Basic Statistic	GLCM	Tile Size (m)	Pixel Pair (m)	Gabor	Wavelength (m)	Angles (deg)	PC	Feature Count
1	Amp, STD, GR	all	1, 2.5	0.1, 0.5	all	0.5, 1, 2	45, 90, 135	-	31
2	Amp, STD, GR	all	1	0.1, 0.5	all	0.5, 1, 2	45, 90, 135	-	20
3	Amp, STD, GR	all	2.5		all	0.5, 1, 2	45, 90, 135	-	20
4	Amp, STD, GR	all	1		all	0.5, 0.8, 1, 1.5, 2, 4	45, 60, 90, 135	-	35
5	Amp	-	1	-	-	-	-	-	1
6	Amp, GR	-	1	-	-	-	-	-	2
7	Amp, STD, GR	-	1	-	-	-	-	-	3
8	-	all	1	0.1, 0.5	-	-	-	-	8
9	GR	all	1	0.1, 0.5	-	-	-	-	9
10	-	-	-	-	all	0.5, 0.8, 1, 1.5, 2, 4	45, 60, 90, 135	-	24
11	-	-	-	-	all	0.8, 1, 1.5, 2	45, 60, 90, 135	-	16
12	-	-	-	-	all	0.8, 1, 1.5, 2	45, 90, 135	-	12
13	-	-	-	-	PC 1 & 2	0.5, 0.8, 1, 1.5, 2, 4	45, 60, 90, 135	-	2
14	-	-	-	-	PC 1, 2 & 3	0.5, 0.8, 1, 1.5, 2, 4	45, 60, 90, 135	-	3
15	Amp, STD	all	1	0.1, 0.5	all	0.5, 0.8, 1, 1.5, 2, 4	45, 60, 90, 135	-	34
16	Amp, STD	all	1	0.1, 0.5	all	0.5, 1, 2	45, 90, 135	-	19
17	Amp, STD	all	1	0.1, 0.5	PC 1 & 2	0.5, 0.8, 1, 1.5, 2, 4	45, 60, 90, 135	-	12
18	Amp, STD, GR	all	1, 2.5	0.1, 0.5	all	0.5, 0.8, 1, 1.5, 2, 4	45, 60, 90, 135	yes	1
19	Amp, STD, GR	all	1, 2.5	0.1, 0.5	all	0.5, 0.8, 1, 1.5, 2, 4	45, 60, 90, 135	yes	3
20	Amp, STD, GR	all	1, 2.5	0.1, 0.5	all	0.5, 0.8, 1, 1.5, 2, 4	45, 60, 90, 135	yes	5
21	Amp, STD, GR	all	1	0.1, 0.5	all	1	45, 90, 135	-	14
22	Amp, STD, GR	all	1	0.1	all	1	45, 90, 135	-	10
23	Amp, STD, GR	all	1	0.1, 0.5	all	0.8	45, 90, 135	-	14
24	Amp, STD, GR	all	1	0.1	all	1	90	-	8

Notes

1. https://nl.mathworks.com/help/images/ref/gabor.html (accessed on 1 November 2024)
2. https://nl.mathworks.com/help/images/ref/graycomatrix.html (accessed on 1 November 2024)

References

1. Van Der Reijden, K.J.; Koop, L.; O'flynn, S.; Garcia, S.; Bos, O.; van Sluis, C.; Maaholm, D.J.; Herman, P.M.; Simons, D.G.; Olff, H.; et al. Discovery of Sabellaria spinulosa reefs in an intensively fished area of the Dutch Contintental Shelf. *J. Sea Res.* **2019**, *144*, 85–94. [CrossRef]
2. Herman, P.M.; van Rees, F. *Mapping Reef Forming North Sea Species*; Deltares: Delft, The Netherlands, 2022.
3. OSPAR. *OSPAR List of Threatened and/or Declining Species and Habitats*; Reference Number: 2008-6; OSPAR: London, UK, 2008.
4. OSPAR_Commision. *Background Document on Sabellaria Spinulosa Reefs*; Biodiversity Series (614/2013); OSPAR: London, UK, 2013.
5. Blondel, P. *The Handbook of Sidescan Sonar*; Springer: Berlin/Heidelberg, Germany, 2009.
6. Lurton, X. *An Introduction to Underwater Acoustics*; Springer: Berlin/Heidelberg, Germany, 2010.
7. Misiuk, B.; Brown, C.J. Benthic habitat mapping: A review of three decades of mapping biological patterns on the seafloor. *Estuar. Coast. Shelf Sci.* **2024**, *296*, 108599. [CrossRef]
8. Gaida, T.C.; Tengku Ali, T.A.; Snellen, M.; Amiri-Simkooei, A.; Van Dijk, T.A.; Simons, D.G. A Multispectral Bayesian Classification Method for Increased Acoustic Discrimination of Seabed Sediments Using Multi-Frequency Multibeam Backscatter Data. *Geosciences* **2018**, *8*, 455. [CrossRef]
9. Steiniger, Y.; Kraus, D.; Miesen, T. Survey on deep learning based computer visio for sonar imagery. *Eng. Appl. Artifical Intellgience* **2022**, *114*, 105157. [CrossRef]
10. Feldens, P.; Darr, A.; Feldens, A.; Tauber, F. Detection of Boulders in Side Scan Sonar Mosaics by a Neural Network. *Geosciences* **2019**, *9*, 159. [CrossRef]
11. Limpenny, D.; Foster-Smith, R.; Edwards, T.; Hendrick, V.; Diesing, M.; Eggleton, J.D.; Meadows, W.J.; Crutchfield, Z.; Pfeifer, S.; Reach, I.S. *Best Methods for Identifying and Evaluating Sabellaria Spinulosa and Cobble Reef*; Natural England: York, UK, 2010.
12. Jenkins, C.; Eggleton, J.; Barry, J.; O'Connor, J. Advances in assessing Sabellaria spinulosa reefs for ongoing monitoring. *Ecol. Evol.* **2018**, *8*, 7673–7687. [CrossRef] [PubMed]
13. Bianconi, F.; Harvey, R.; Wang, W. A texture analysis approach to identifying Sabellaria Spinulosa colonies in sidescan sonar imagery. In Proceedings of the Irish Machine Vision and Image Processing Conference, Galway, UK, 30 August–1 September 2011.
14. Gaida, T.; Binnerts, B.; van der Stappen, C.; Cuperus, J. *Sabellaria Monitoring Trial: Summary Report (id56-Sabellaria-Monitoring-Trial-Summary-Report)*; TNO: The Hague, The Netherlands, 2023.
15. Lurton, X.; Lamarche, G. Backscatter Measurements by Seafloor-Mapping Sonars. Guidelines and Recommendations. 2015. Available online: https://www.researchgate.net/profile/Geoffroy-Lamarche/publication/275890570_Backscatter_measurements_by_seafloor-mapping_sonars_-_Guidelines_and_Recommendations/links/5548dbbb0cf25a87816aa8c8/Backscatter-measurements-by-seafloor-mapping-sonars-Guidelines-and-Recommendations.pdf (accessed on 15 October 2024).
16. Gaida, T.C. *Acosutic Mapping and Monitoring of the Seabed: From Single-Frequency to Multispectral Multibeam Backscatter*; Delft University of Tecnology: Delft, The Netherlands, 2020.
17. van der Reijden, K.J.; Koop, L.; Mestdagh, S.; Snellen, M.; Herman, P.M.J.; Olf, H.; Govers, L.L. Conservation Implications of Sabellaria spinulosa Reef Patches in a Dynamic Sandy-Bottom Environment. *Front. Mar. Sci.* **2021**, *8*, 642659. [CrossRef]
18. Gaida, T.C. Onderzoek naar Zeebodem in de Noordzee, De Rijke Noordzee. 2020. Available online: https://www.derijkenoordzee.nl/nieuws/onderzoek-naar-zeebodem-in-de-noordzee (accessed on 1 October 2024).
19. Gubbay, S. *Defining and Managing Sabellaria spinulosa Reefs: Report of an Inter-Agency Workshop*; JNCC: Peterborough, UK, 2007.
20. Christianini, N.; Shawe-Taylor, J. *An Introduction to Support Vector Machines and Other Kernel-Based Learning Methods*; Cambridge University Press: Cambridge, UK, 2000.
21. Lakshmi, M.D.; Murugan, S.; Padmapriya, N.; Somasekar, M. Texture Analysis on Side Scan Sonar images using EMD, XCS-LBP and Statistical Co-occurrence. In Proceedings of the 2019 International Symposium on Ocean Technology, Ernakulam, India, 11–13 December 2019.
22. Febriawan, H.K.; Helmholz, P.; Parnum, I.M. Support vector machine and decision tree based classification of side-scan sonar mosaics using textural features. In *The International Archives of the Photogrammetry*; Remote Sensing and Spatial Information Sciences: Enschede, The Netherlands, 2019.
23. Solikin, S.; Munandar Manik, H.; Pujiyati, S. Support Vector Machine Classification Method for Predicting Jakarta Bay Bottom Sediment Type using Multibeam Echosounder Data. *Sci. Technol.* **2020**, *28*, 477–491.
24. *Data Managment Factsheet: Monitoring Onderzoek Natuurversterking Soortenbescherming (31190788)*; Witteveen & Bos: Deventer, The Netherlands, 2024.

25. Gaida, T.C.; Binnerts, B.; Cuperus, J.; Bos, O.; van der Jagt, H. *Presence of Sabellaria Spinulosa Reefs in the Northern Brown Bank, Dutch Continental Shelf, North Sea (MONS ID56: Monitoring Reef-Building Species)*; TNO: Den Haag, The Netherlands, 2024.
26. Bos, O.G.; Coolen, J.W.P.; van der Wal, J.T. *Biogene Riffen in de Noordzee. Actuele en Potentiele Verspreiding van Rifvormende Schelpdieren En Wormen (C058/19)*; Wageningen Marine Research: Yerseke, The Netherlands, 2019.
27. Ying, X. An overview of overfitting and its solutions. *J. Phys. Conf. Ser.* **2019**, *1168*, 022022. [CrossRef]
28. Zhu, P.; Isaacs, J.C.; Fu, B.; Ferrari, S. Deep learning feature extraction for target recognition and classification in underwater images. In Proceedings of the 2017 IEEE 56th Annual Conference on Decision and Control (CDC), Melbourne, VIC, Australia, 12–15 December 2017.
29. McKay, J.; Gerg, I.; Monga, V.; Raj, R.G. What's mine is yours: Pretrained CNNs for limited training sonar ATR. In Proceedings of the Oceans 2017, Anchorage, AK, USA, 19–22 June 2017.
30. Luo, X.; Qin, X.; Wu, Z.; Yang, F.; Wang, M.; Shang, J. Sediment Classification of Small-Size Seabed Acoustic Images Using Convolutional Neural Networks. *IEEE Access* **2019**, *7*, 98331–98339. [CrossRef]
31. Zhang, H.; Zhao, J.; Yang, K. Study on the Fusion of MBS Image and SSS Image. In Proceedings of the OCEANS'10 IEEE, Sydney, Australia, 24–27 May 2010.
32. Zhao, J.; Meng, J.; Zhang, H.; Yan, J. A new method for acquisition of high-resolution seabed topography by matching seabed classification images. *Remote Sens.* **2017**, *9*, 1214. [CrossRef]